Vacuum Ultraviolet Excitation of Large Water Clusters

M. Ahmed, C. J. Apps, C. Hughes, and J. C. Whitehead*

Department of Chemistry, University of Manchester, Manchester M13 9PL, U.K.

Received: August 24, 1994[⊗]

The fluorescence excitation spectrum of water clusters containing up to 1500 water molecules has been studied using synchrotron radiation in the spectral region 60−250 nm. Fluorescence is only observed for excitation of the water clusters in the region 100−140 nm. Water clusters do not fluoresce for excitation wavelengths lower or higher than this range. The fluorescence lies in the spectral region 200−420 nm and is peaked at 300−350 nm. The fluorescence excitation spectrum closely resembles that for free water molecules, and we see no shifts in the spectrum relative to gaseous molecules. It is suggested that the fluorescence comes from Rydberg-excited water molecules lying at the surface of the cluster that are photodetached and predissociate into fluorescent fragments. Below 100 nm, the clusters photoionize to give protonated cluster ions rather than electronically excited monomer ions as in the gas phase. We see no evidence for emission similar to that recently reported for UV excitation of ice crystals [Matich, A. J.; *et al. J. Phys. Chem.* **1993**, *97*, 10539].

Introduction

The use of clusters as a medium for studying molecular systems allows an investigation of how the bulk properties of a substance emerge from the properties of an isolated molecule as the cluster size increases. Molecular beam methods have been used to generate and characterize large clusters of water molecules formed in supersonic expansions.[1,2] The photophysics and photochemistry of liquid and solid water have great importance in a wide range of environments ranging from biological systems to the chemistry of the earth's atmosphere and interstellar space. It is well-known that isolated water molecules in the gas phase absorb radiation below 176 nm and that fluorescence is observed for excitation wavelengths below 136.7 nm.[3,4] The long-wavelength threshold for absorption shifts to 150 nm for liquid water[5] and to 157 nm for ice (both amorphous and hexagonal crystalline forms).[6] These blue shifts in going from the isolated gas-phase molecule correspond to energies about twice that of the hydrogen bond strength in water. Onaka and Takahashi[7] have measured the absorption spectra for liquid water and ice down to 100 nm. The major dissociation products following the photoexcitation of water with wavelengths above the ionization limit (98 nm) are H atoms and OH radicals in the gas phase and for ice[8] but include the hydrated electron, hydroxyl radical, and proton for the photolysis of liquid water.[5]

Fluorescence has been observed from UV-excited ice (220−250 nm), giving emission peaking at 340 and 420 nm.[9,10] The emission is composed of a long-lived component ($\tau \approx 1.3$ s) peaking at ~420 nm and a shorter lived component ($\tau < 30$ ms) at the shorter emission wavelength. The short-lived emission system is assigned to either the Herzberg I or III system of O_2, which is thought to be chemically formed in the ice. An assignment of the long-lived emission has not been made. A similar emission at ~420 nm has been observed in UV-excited alkaline ices,[11−13] and the emitter has been variously assigned to OH* or an exciplex of atomic hydrogen with water $[(H_2O)_nH]^*$. Fluorescence has also been observed[14] following electron impact excitation of ice, which is attributed to OH-$(A^2\Sigma^+ \rightarrow X^2\Pi)$ emission.

In this article, we report the study of the photoexcitation of large water clusters ($\bar{n} \leq 1500$) generated in a supersonic molecular beam expansion using synchrotron radiation where we monitored the production of fluorescence. Synchrotron radiation has previously been used[15] to study the photoionization of water clusters producing small water cluster ions of the type $(H_2O)_2^+$, $(H_2O)_3^+$, $(H_2O)_2H^+$ and $(H_2O)_3H^+$. In addition, weak visible and ultraviolet fluorescence has been observed[16] from the excitation of water clusters ($\bar{n} \leq 1000$) by impact with 90 eV electrons without any spectral determination of the identity of the emitters. We know of no reported studies of the fluorescence resulting from synchrotron-excited water clusters.

Experimental Section

A. Apparatus. Water clusters were produced by the supersonic expansion of pure water vapor from a temperature-controlled reservoir (<420 K) through a 0.3 mm conical nozzle, giving stagnation pressures, P_0, up to 3 bar. The temperature of the nozzle was maintained a few degrees hotter than the reservoir and lead tubes. The vacuum chamber was constructed from standard vacuum components and had an internal diameter of ~100 mm. The water vapor was pumped by an arrangement of high-efficiency cryopanels (surface area 0.13 m^2) cooled by flowing liquid nitrogen. The chamber was evacuated by a turbomolecular pump, and with the cryopumping, a base pressure of 1×10^{-5} mbar and a typical pressure of 5×10^{-5} mbar with the beam running were achieved. The vacuum UV radiation of the synchrotron in the spectral region 60−250 nm (Daresbury SRS, Station 3.1), operating in multibunch mode, was dispersed by a 1 m Seya Namioka monochromator with an effective resolution of ~8 Å scanned with a step size of 4 Å. The radiation entered the chamber *via* a quartz capillary tube (1 mm i.d.) acting as a light-guide and then intersected the cluster beam at right angles close to the nozzle. The resulting fluorescence was observed at right angles to both the cluster and synchrotron beams *via* a quartz window, and a filter and was focused on to the photocathode of a pulse-counting photomultiplier (EMI 9883QKA, $\lambda > 200$ nm) by a quartz lens (38 mm diameter, 45 mm focal length). Color glass filters (Schott WG225 and GG420) were used to isolate the fluorescence. Fluorescence signals were typically 3.8×10^4 counts s^{-1} at the peak compared with $< 2 \times 10^3$ counts s^{-1} resulting from background water vapor at 5×10^{-5} mbar. The signals were corrected for any contribution due to background fluorescence.

[⊗] Abstract published in *Advance ACS Abstracts*, November 1, 1994.

0022-3654/94/2098-12530$04.50/0

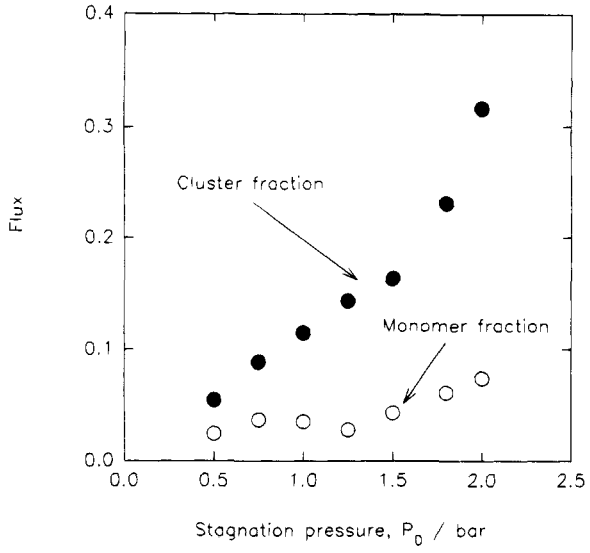

Figure 1. Relative fluxes of water monomers and clusters as a function of the stagnation pressure, P_0, for a conical nozzle of diameter 0.3 mm.

B. Characterization of the Water Cluster Beam. Further experiments were performed to characterize the properties of the water cluster beam. For these experiments, the cluster beam source was mounted in another molecular beam apparatus equipped with differential pumping provided by oil diffusion pumps and liquid nitrogen cryopumping.[17] Three different types of experiment were performed. Firstly, the velocity distributions of the monomer and the various cluster components of the beam were measured by time-of-flight where the beam was chopped by a rotating slotted disk (12.6 ms period, 120 μs open time). After a flight path of 486 mm, the chopped beam was ionized and mass analyzed by a quadrupole mass filter (VSW Mass Analyst 0−300 amu, 1 mA emission, 70 eV electron energy). The peak velocity is highest for the monomer (~1100 m s^{-1}) and decreases with increasing cluster size to a constant value (~950 m s^{-1}). The translational temperature of the monomers and smaller clusters in the beam is ~105 K. These results closely parallel those of Dreyfuss and Wachman.[1] When the quadrupole is set on the monomer mass peak, we observe a bimodal structure to the velocity distributions. The slow component comes from water clusters that fragment in the ionizer and the faster component results from monomers. This behavior has previously been reported for large clusters of argon[18] and N_2O.[19] Cuvellier and Binet have shown[18] how it is possible to determine the ratio of free monomers to clusters in the beam by integrating the areas of the two components in the bimodal velocity distribution. In Figure 1, we show the ratio of the flux of water monomers to that of the clusters as a function of the stagnation pressure of water vapor in the source. At low pressures (<0.5 bar) the beam is mainly composed of monomers, but at higher pressures condensation readily occurs and the flux of clusters rapidly increases. This onset of clustering is confirmed by Pitot tube measurements of the total flux of the beam where the clusters are broken up by collisions with the wall and ionization gauge pressure measurements yield the total flux. This curve is shown in Figure 2, and the change in slope at a stagnation pressure of ~1.6 bar is identified with the formation of large clusters.

The relative intensities of the different sized water clusters can be measured at low stagnation pressures using the quadrupole mass spectrometer which can detect the smaller water clusters, $(H_2O)_n$, up to $n = 16$. The relative intensity distribution as a function of cluster size is found to fall exponentially for the smallest cluster sizes. This type of distribution is indicative of clustering *via* successive addition of monomers stabilized by three-body collisions.[20] As the stagnation pressure is increased, it is no longer possible to measure the cluster size distribution using the quadrupole mass spectrometer. Instead, we determine the distribution using a time-of-flight method in which the beam is pulse ionized by an electron beam (10 μs pulse width), extracted at an energy of 11 eV, and detected by an electron multiplier after a flight path of 15.23 cm. The resulting cluster size distributions are shown in Figure 3 for three stagnation pressures. These distributions show the approximately bell-shaped form that is characteristic of the formation of large clusters by coalescence resulting from cluster−cluster collisions[21] where the newly formed clusters are stabilized by evaporative cooling. It can be seen that, for a stagnation pressure of 2.4 bar, we have a distribution with $\bar{n}$ ~

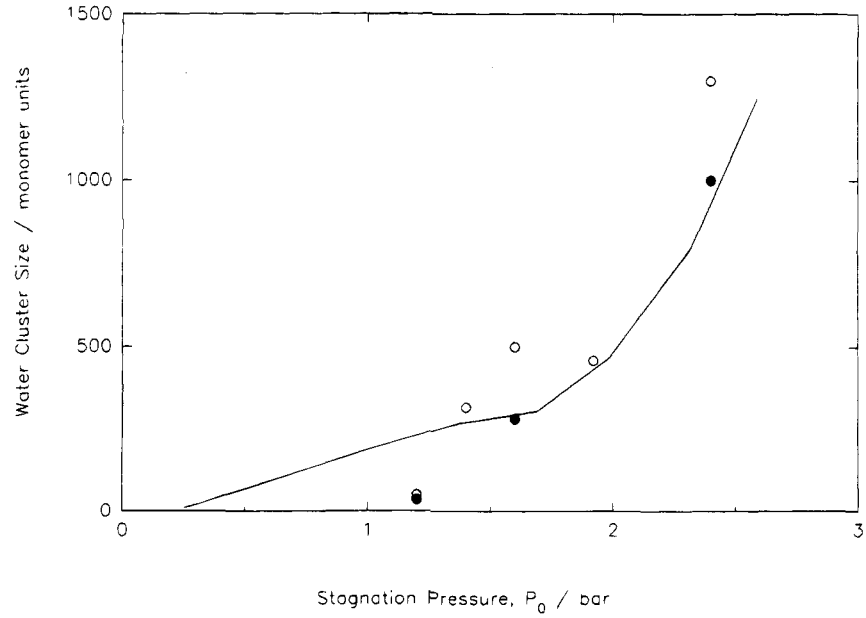

Figure 2. Size distribution of the water cluster beam as a function of the stagnation pressure, P_0, for a conical nozzle of diameter 0.3 mm (open circles). The results are compared with the scaled results of Torchet *et al.*[2] (sonic nozzle, 0.4 mm diameter) (filled circles). The solid curve represents the Pitot tube measurement of the total flux for the beam.

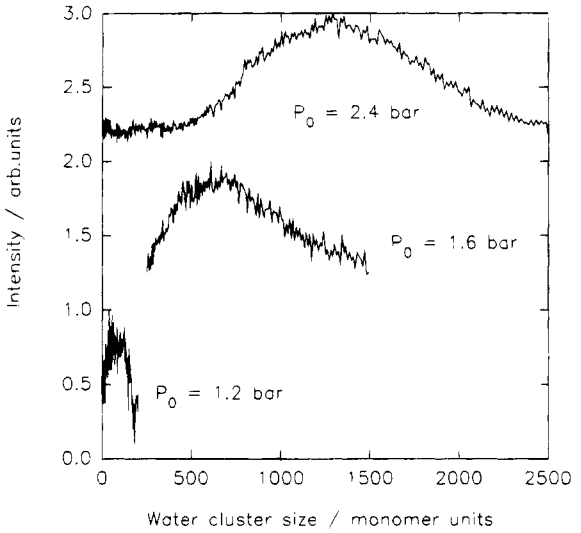

Figure 3. Cluster size distributions measured by the time-of-flight method for stagnation pressures, P_0, = 1.2, 1.6, and 2.4 bar.

1300 and a full width at half maximum of ~1000 monomer units. Using electron diffraction methods, Torchet *et al.*[2] have shown that clusters of a few hundred water molecules have an amorphous crystalline structure whilst clusters composed of several thousand water molecules exhibit a diamond cubic form with a mean diameter of ~4.5 nm for a cluster containing ~1500 monomers, assuming a spherical shape for the cluster. This is probably an inappropriate approximation, as the cluster will exhibit some structural irregularities. Clusters formed from pure water expansions are found to reach a limiting internal temperature of 180 K.[2]

It has been shown[22] that for large clusters of atoms and molecules, the mean cluster sizes can be related by a scaling law of the form

$$P_0 D_{\text{eff}}^{1.5} T_0^{-2.4} = \text{const} \qquad (1)$$

where D_{eff} is the effective nozzle diameter taking into account the nozzle geometry and T_0 is the reservoir gas temperature. We find that this relationship applies well to our water cluster beams, and on Figure 2 we show the comparison between our determinations of mean cluster size as a function of stagnation pressure and the scaled results of Torchet *et al.*[2] Equation 1 can then be used to predict cluster size for other source conditions. Vostrikov *et al.*[23] have also investigated the use of scaling laws similar to eq 1 for water clusters.

Results

We have measured the fluorescence excitation spectrum resulting from the interaction of the water cluster beam with synchrotron radiation between 60 and 250 nm for a range of stagnation pressures up to 3.0 bar corresponding to variations in the cluster size distributions as discussed above. A typical fluorescence excitation spectrum is shown in Figure 4 for a source stagnation pressure of ~2.5 bar. The form of this spectrum is very similar to that obtained for water vapor,[4] and there are no detectable spectral shifts in the positions of the peaks in the spectrum with varying source pressure. At our resolution (~8 Å), this means that any shift is less than 550 cm^{-1}. However, we find that the variation of the intensity of the fluorescence with source stagnation pressure for excitation at a particular wavelength is not the same for all excitation wavelengths. This is illustrated in Figure 5. No fluorescence is observed for excitation wavelengths greater than ~140 nm,

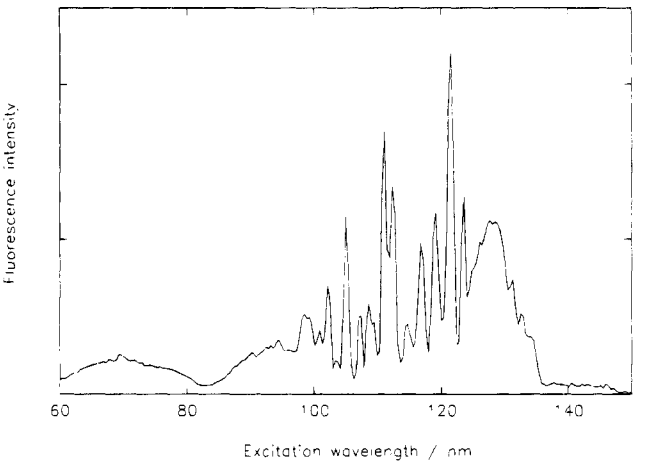

Figure 4. Fluorescence excitation spectrum recorded for a water cluster beam with a residual monomer contribution for a stagnation pressure of $P_0 = 2.5$ bar. The spectrum was recorded for excitation wavelengths in the range 60−150 nm with a resolution of 0.8 nm.

close to the long-wavelength threshold for fluorescence from gas-phase water. In addition, by using filters, we find that the spectrum of the fluorescence peaks at ~300−350 nm and does not extend beyond 420 nm.

Discussion

As noted above, the form of the fluorescence excitation spectrum measured for the water cluster beam closely resembles that previously measured for gas-phase water molecules. For gaseous water, the fluorescence results from the 306.4 nm A → X emission system of OH, which is formed by predissociation of highly excited Rydberg states of H_2O for excitation wavelengths above the ionization threshold (98.4 nm). Below ~83 nm, the fluorescence is thought[4] to result from the electronically-excited $\tilde{A}$ and $\tilde{B}$ states of H_2O^+ formed by photoionization. Figure 5 shows that the variation of fluorescence intensities with stagnation pressure depends on the excitation wavelength. In general, the intensity of the fluorescence resulting from excitation at wavelengths greater than 100 nm rises more rapidly than that at lower excitation wavelengths. The form of these curves should be compared with the estimates of the fluxes of the monomer and cluster components of the beam shown in Figure 1. It can be seen that the flux of the monomer fraction rises by only a factor of 3 in going from a stagnation pressure of 0.5 to 2.0 bar, whilst the flux of clusters increases by ~6. Thus, for excitation wavelengths greater than 100 nm, the observed fluorescence would seem to result from excitation of water clusters, but below this wavelength only the monomer portion of the beam contributes to the fluorescence.

We do not observe any similarities in our fluorescence excitation spectra with the results from the UV excitation of ice[9,10] despite our clusters being crystalline in character. We do not observe any fluorescence for excitation wavelengths greater than 140 nm, whilst fluorescence has been observed from ice for excitation wavelengths of 220−250 nm. In addition, we have no evidence for any emission peaking at 420 nm, as was observed for the long-lived component of the emission from UV-excited ice. However, it should be noted that the geometry of our crossed cluster and synchrotron beams and the focused fluorescence detection arrangement restrict the lifetime of any emission that we observe to a maximum of ~10 μs before the emitter has been carried out of the observation region in the beam. The wavelength dependence of the fluorescence would seem to indicate that it originates from OH(A) → OH(X) emission similar to that observed for the corresponding excita-

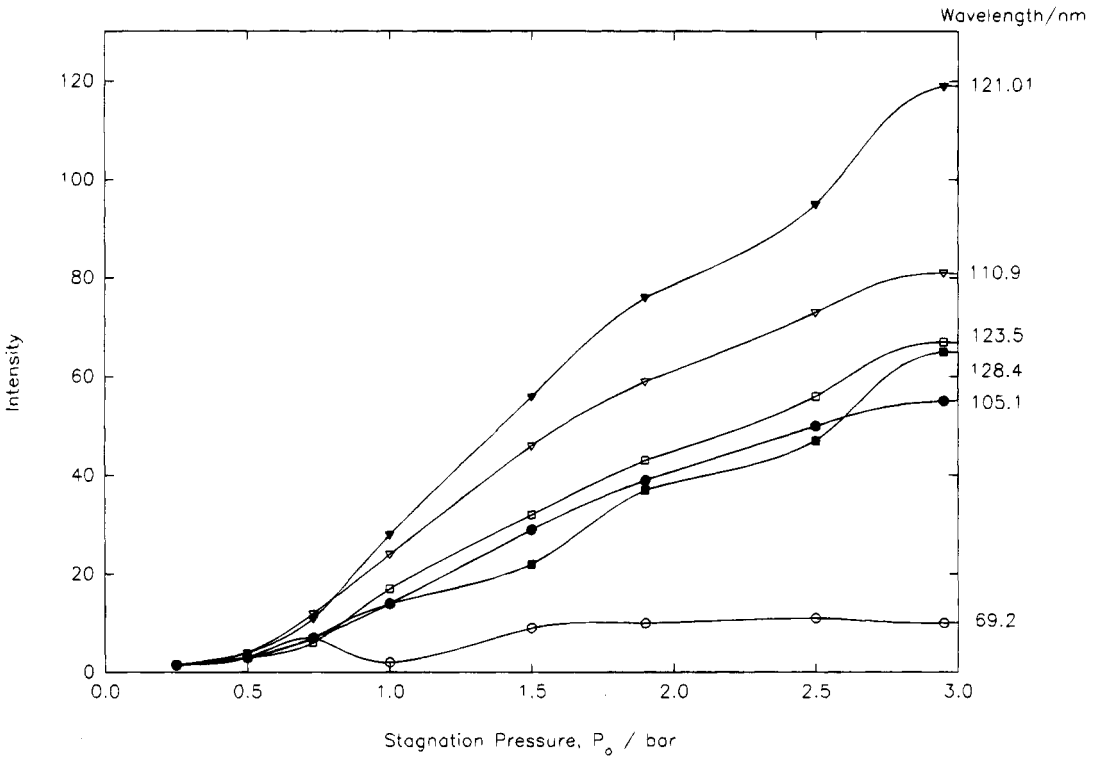

Figure 5. Variation of the intensity of fluorescence as a function of the stagnation pressure, P_0, recorded for excitation wavelengths of 69.2, 105.1, 110.9, 121.01, 123.5, and 128.4 nm.

tion of gaseous water. The character of these Rydberg states in the water cluster will be considerably changed from those in the isolated molecule, and there will be a shift in the electronic absorption spectrum to higher frequency. There is an exciton transition in the absorption spectrum of liquid water at 8.3 eV (149 nm) attributed to the $1b_1 \rightarrow 3s$ Rydberg transition, which is shifted to 8.5 eV (146 nm) in ice. The corresponding transition occurs at 7.44 eV (167 nm) in the gas phase;[24] a shift of over eight thousand wavenumbers in going from gas to solid phase. As we do not see a shift in excess of 550 cm^{-1}, we can say that we are not exciting molecules in the bulk ice-like part of the cluster.

Perhaps the closest analogy to our work comes from the studies by Nishi *et al.*[25] on the photodetachment and photodissociation of surface molecules from water ice films by UV radiation. They point out that there is an essential difference between surface molecules and molecules in the bulk. The edge molecules are only weakly bound to the crystal with consequently less lowering of the Rydberg energy levels. The photon energy absorbed by the cluster is rapidly transferred from the inside of the cluster to the surface molecule, which then becomes photodetached in an excited state, dissociating to give OH(A) and H on leaving the surface. We can then represent the process as follows

$$(H_2O)_n + h\nu \rightarrow (H_2O)_n^* \rightarrow (H_2O)_{n-1} + H_2O^* \rightarrow (H_2O)_{n-1} + OH(A)^* + H \quad (2)$$

where the elimination of a single molecule from the cluster is the most energetically favored dissociation process. Vostrikov *et al.*[16] similarly assign the emission that they observe from the electron-excited water clusters to the elimination of an electronically-excited molecule. Berry[26] has also discussed another possible difference between molecules in the surface layer and the bulk, where there can be two coexisting phase-like forms (*e.g.* a liquid-like surface layer and a solid-like core) which might influence the photodetachment process. The surface of the water cluster is likely to be less regular than that of an ice film. Molecular dynamics calculations[27] for water clusters with ~500 water molecules indicate that there are considerable surface irregularities with an abundance of nonbonding or "dangling" OH groups. Nishi *et al.*[25] have shown that the efficiency of photodetachment from their water ice films is enhanced by surface roughness and that annealing the surface reduces that efficiency. The energy required to dissociate a water molecule from the cluster will be lost to the photodetached water molecule, and we might expect that the relative translational energy or the internal energy of the departing OH will differ from that observed in the photodissociation of free water molecules. It would be interesting to investigate this hypothesis experimentally using photofragment translational or emission spectroscopy.

For excitation wavelengths below 100 nm, we do not find any evidence for UV-induced emission from water clusters, in contrast to the situation with free water molecules, where there is emission from H_2O^+ ($\tilde{A}$ and $\tilde{B}$) albeit with a relatively low quantum yield (~2%).[4] Photoionization studies have been performed on small water clusters using Ar resonance radiation (104.8 and 106.7 nm)[28] and synchrotron radiation (80 and 107–116 nm),[15] investigating the nature of the ions observed and measuring their appearance potentials which are ~11 eV, depending on the size of the cluster. For pure water clusters, protonated cluster ions are observed following a rapid intracluster proton transfer process of the type

$$(H_2O)_n + h\nu \rightarrow [(H_2O)_n^+]^* + e^- \rightarrow (H_2O)_{n-1}H^+ + OH + e^- \quad (3)$$

Whilst there is evidence for some further fragmentation of the initially produced ion, $[(H_2O)_n^+]^*$,

$$(H_2O)_n + h\nu + [(H_2O)_n^+]^* + e^- \rightarrow (H_2O)_{n-m-1}H^+ + OH + mH_2O + e^- \quad (4)$$

this is not thought to be excessive (m is <3) and the excess energy of process 4 is low. Thus, there would not appear to be any possibility of forming electronically excited H_2O^+ by subsequent fragmentation following photoionization of our large water clusters. This offers an explanation for our observation of no fluorescence from the water clusters for excitation below the ionization threshold. The only fluorescence at these excitation wavelengths that we observe can be correlated with the residual monomer component of the beam.

Conclusions

Using a supersonic expansion of pure water vapor, we have generated large clusters containing up to 1500 water molecules. We observed fluorescence in the spectral region 200−420 nm, peaked at 300−350 nm, from excitation of the water clusters by synchrotron radiation in the range 100−140 nm. Water clusters do not fluoresce for excitation wavelengths lower or higher than this range. The fluorescence excitation spectrum closely resembles that for free water molecules, and we see no shifts in the spectrum relative to gaseous molecules. We suggest that the fluorescence comes from Rydberg-excited water molecules that lie at the surface of the cluster becoming photodetached and predissociating into fluorescent fragments. Below 100 nm, the clusters will photoionize to give protonated cluster ions rather than electronically excited monomer ions. We see no evidence for emission similar to that reported for UV excitation of ice crystals.

Acknowledgment. The authors wish to thank the staff of the Daresbury Laboratory for their help, particularly Drs. A. Hopkirk and M. A. MacDonald and Mr. C. Mythen. This work was supported by EPSRC and NERC.

References and Notes

(1) Dreyfuss, D.; Wachman, H. Y. *J. Chem. Phys.* **1982**, *76*, 2031.
(2) Torchet, G.; Schwartz, P.; Farges, J.; de Feraudy, M. F.; Raoult, B. *J. Chem. Phys.* **1983**, *79*, 6196.
(3) Lee, L. C. *J. Chem. Phys.* **1980**, *72*, 4334.
(4) Lee, L. C.; Suto, M. *Chem. Phys.* **1986**, *110*, 161.
(5) Boyle, J. W.; Ghormley, J. A.; Hochanadel, C. J.; Riley, J. F. *J. Phys. Chem.* **1969**, *73*, 2886.
(6) Dressler, K.; Schnepp, O. *J. Chem. Phys.* **1960**, *33*, 270.
(7) Onaka, R.; Takahashi, T. *J. Phys. Soc. Jpn.* **1968**, *24*, 548.
(8) Ghormley, J. A.; Hochanadel, C. J. *J. Phys. Chem.* **1971**, *75*, 40.
(9) Quickenden, T. J.; Litjens, R. A. J.; Freeman, C. G.; Trotman, S. M. *Chem. Phys. Lett.* **1985**, *114*, 164.
(10) Matich, A. J.; Bakker, M. G.; Lennon, D.; Quickenden, T. I.; Freeman, C. G. *J. Phys. Chem.* **1993**, *97*, 10539.
(11) Maria, H. J.; McGlynn, S. P. *J. Chem. Phys.* **1970**, *52*, 3402.
(12) Merkel, P. B.; Hamill, W. H. *J. Chem. Phys.* **1971**, *55*, 2174.
(13) Mathers, T. L.; Nauman, R. V.; McGlynn, S. P. *Chem. Phys. Lett.* **1986**, *126*, 408.
(14) Miyazaki, T.; Nagasaka, S.; Kamiya, Y.; Tanimura, K. *J. Phys. Chem.* **1993**, *97*, 10715.
(15) Shiromaru, H.; Shinohara, H.; Washida, N.; Yoo, H.-S.; Kimura, K. *Chem. Phys. Lett.* **1987**, *141*, 7.
(16) Vostrikov, A. A.; Gilyova, V. P.; Dubov, D. Yu. *Z. Phys. D* **1991**, *20*, 205.
(17) Dutton, N. J.; Fletcher, I. W.; Whitehead, J. C. *Mol. Phys.* **1984**, *52*, 475.
(18) Cuvellier, J.; Binet, A. *Rev. Phys. Appl.* **1988**, *23*, 91.
(19) Visticot, J. P.; Mestdagh, J. M.; Alcaraz, C.; Cuvellier, J.; Berlande, J. *J. Chem. Phys.* **1988**, *88*, 3081.
(20) Haberland, H. In *Clusters of Atoms and Molecules; Theory, Experiment and Clusters of Atoms*; Haberland, H., Ed.; Springer-Verlag: Berlin, 1994; p 207.
(21) Soler, J. M.; García, N.; Echt, O.; Sattler, K.; Recknagel, E. *Phys. Rev. Lett.* **1982**, *49*, 1857.
(22) Obert, W. In *11th Symposium on Rarified Gas Dynamics*; Campargue, R., Ed.; Commissariat à L'Energie Atomique: Paris, 1979; p 1181.
(23) Vostrikov, A. A.; Dubov, D. Yu.; Predtechenskii, M. R. *Sov. Phys.—Tech. Phys.* **1986**, *31*, 821.
(24) Gürtler, P.; Saile, V.; Koch, E. E. *Chem. Phys. Lett.* **1977**, *51*, 386.
(25) Nishi, N.; Shinohara, H.; Okuyama, T. *J. Chem. Phys.* **1984**, *80*, 3898.
(26) Berry, R. S. *J. Phys. Chem.* **1994**, *98*, 6910.
(27) Hixson, H. G.; Wojcik, M. J.; Devlin, M. S.; Devlin, J. P.; Buch, V. *J. Chem. Phys.* **1992**, *97*, 753.
(28) Shinohara, H.; Nishi, N.; Washida, N. *J. Chem. Phys.* **1986**, *84*, 5561.